PET Imaging of Tumours with a ^{64}Cu Labeled Macrobicyclic Cage Amine Ligand Tethered to Tyr^3-Octreotate

Brett M. Paterson,[a,b] Peter Roselt,[c] Delphine Denoyer,[c] Carleen Cullinane,[c,d] David Binns,[e] Wayne Noonan,[c] Charmaine M. Jeffery,[f] Roger I. Price,[f,g] Jonathan M. White,[a,b] Rodney J. Hicks*,[d,e] and Paul S. Donnelly*,[a,b]

[a]School of Chemistry, [b]Bio21 Molecular Science and Biotechnology Institute and [d]The Sir Peter MacCallum Department of Oncology, The University of Melbourne, Parkville, VIC, Australia
[c]Research Division and [e]Centre for Cancer Imaging, Peter MacCallum Cancer Centre, St Andrews Pl, East Melbourne, VIC, Australia
[f]Department of Medical Technology and Physics, Sir Charles Gairdner Hospital, Nedlands, WA, Australia.
[g]School of Physics, The University of Western Australia, Nedlands, WA, Australia

E-mail: pauld@unimelb.edu.au, Rod.Hicks@petermac.org

***To whom correspondence should be addressed.**

Table of Contents

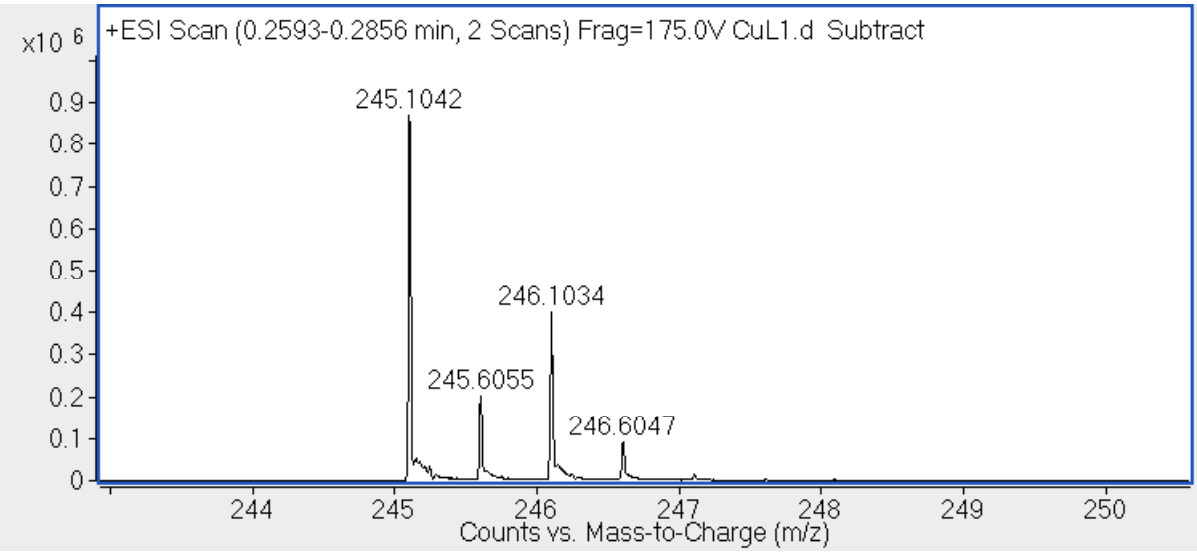

Figure S1: ESI-MS spectrum of $[Cu(MeCOSar)](ClO_4)_2 \cdot 0.5(HClO_4)$

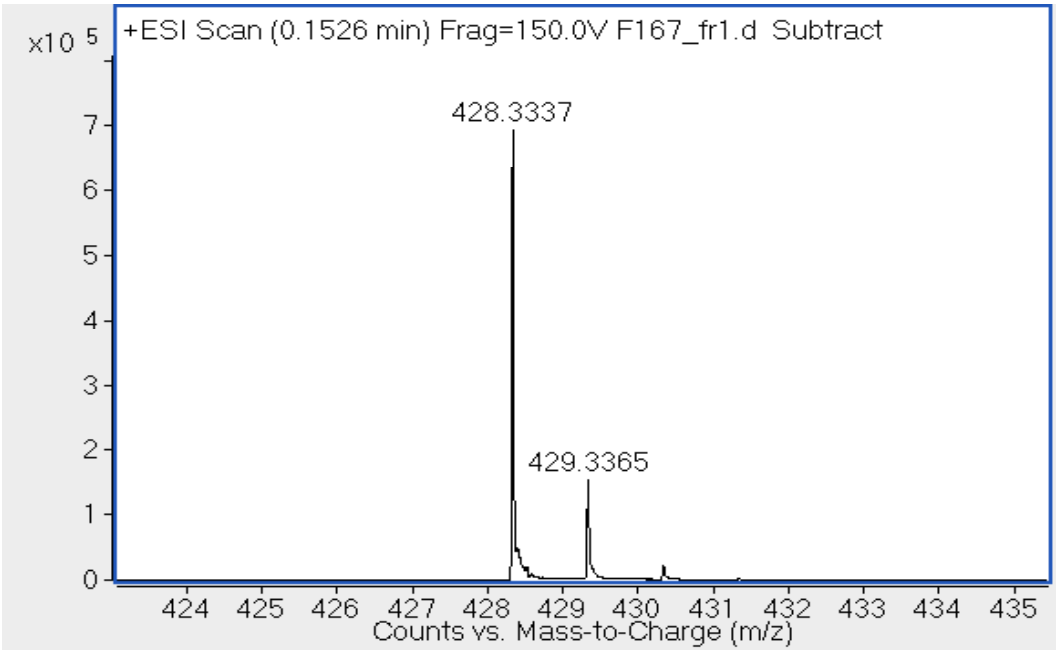

Figure S2: ESI-MS spectrum of MeCOSar·xHCl·xH_2O

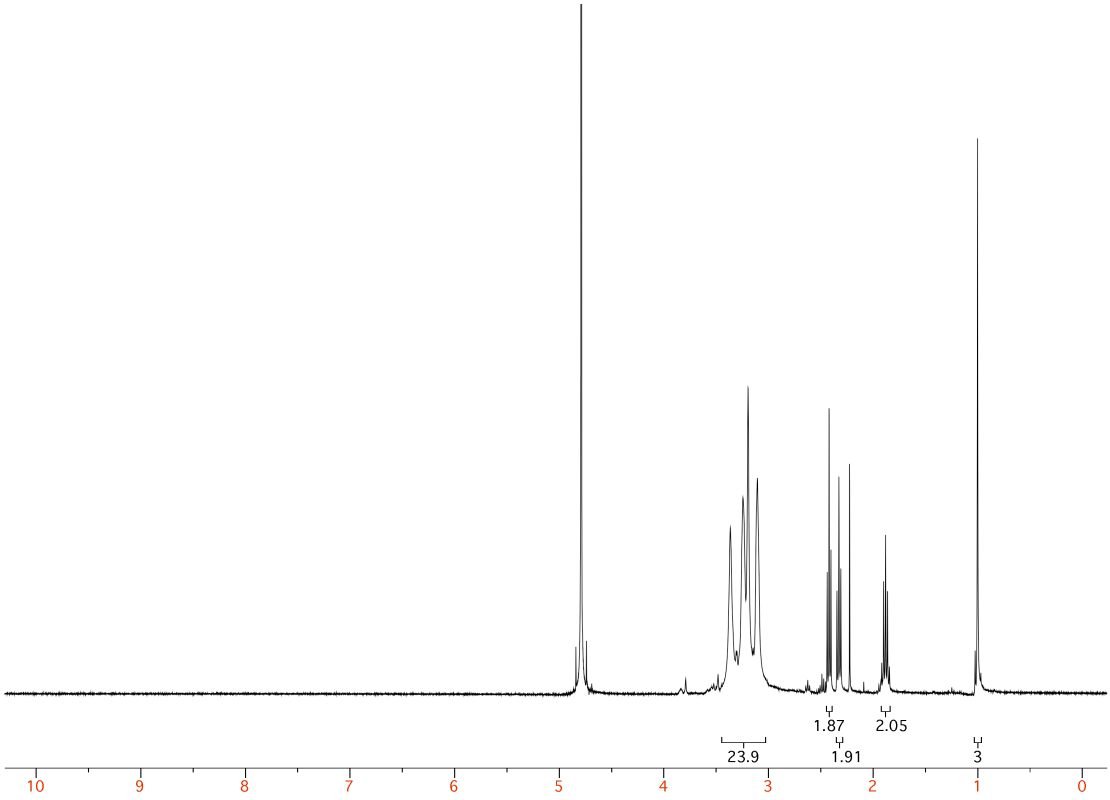

Figure S3: ^{1}H NMR spectrum of MeCOSar·xHCl·xH_2O

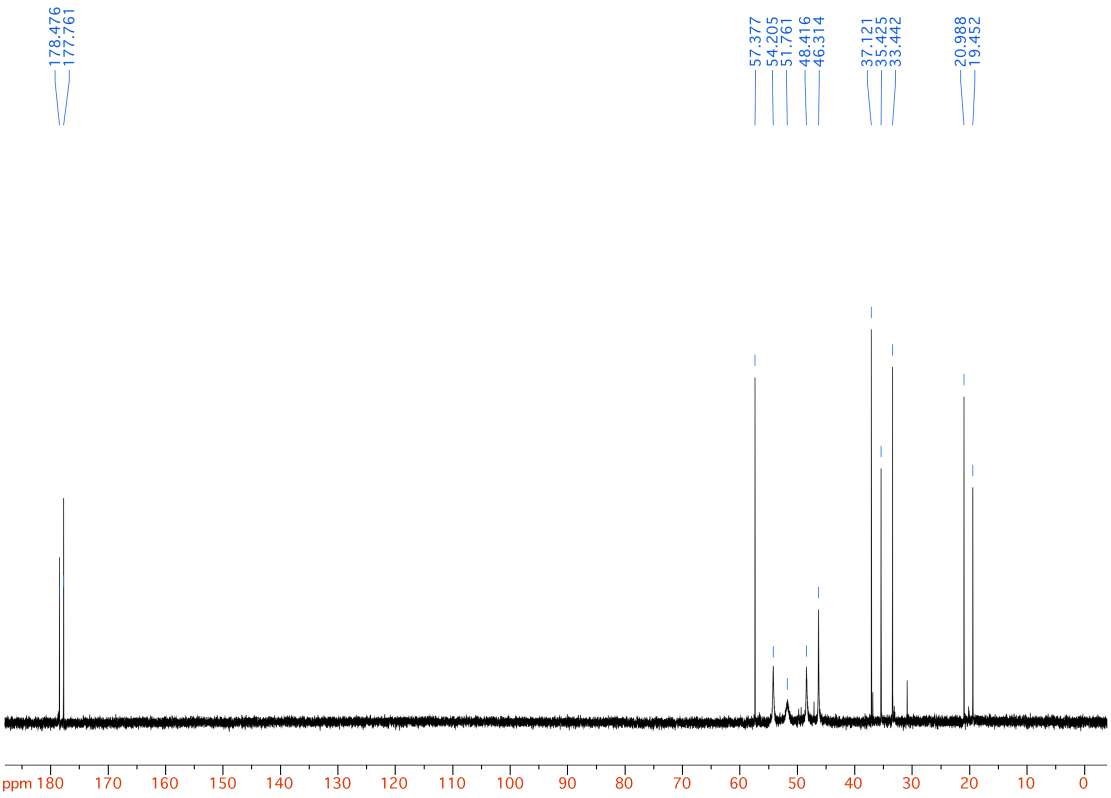

Figure S4: ^{13}C NMR spectrum of MeCOSar·xHCl·xH_2O in D_2O

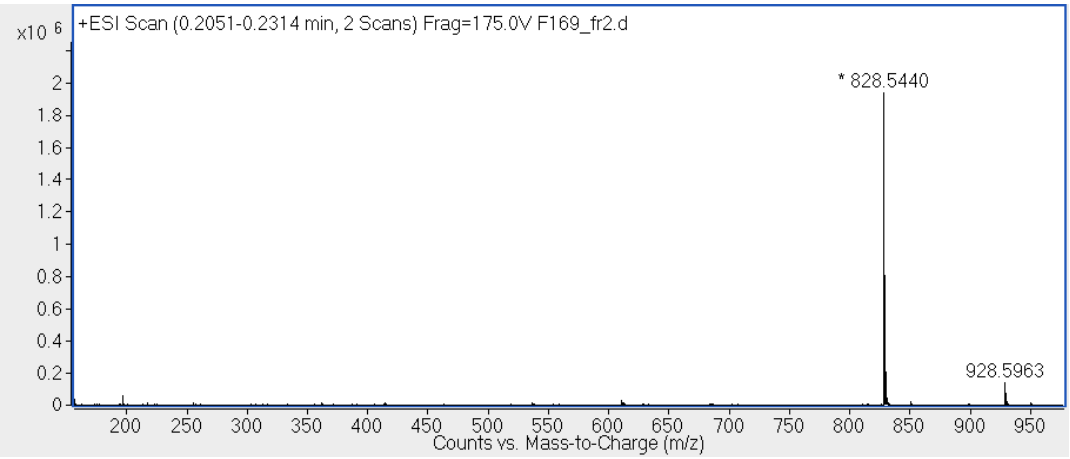

Figure S5: ESI-MS spectrum of (t-Boc)$_{4\text{-}5}$MeCOSar

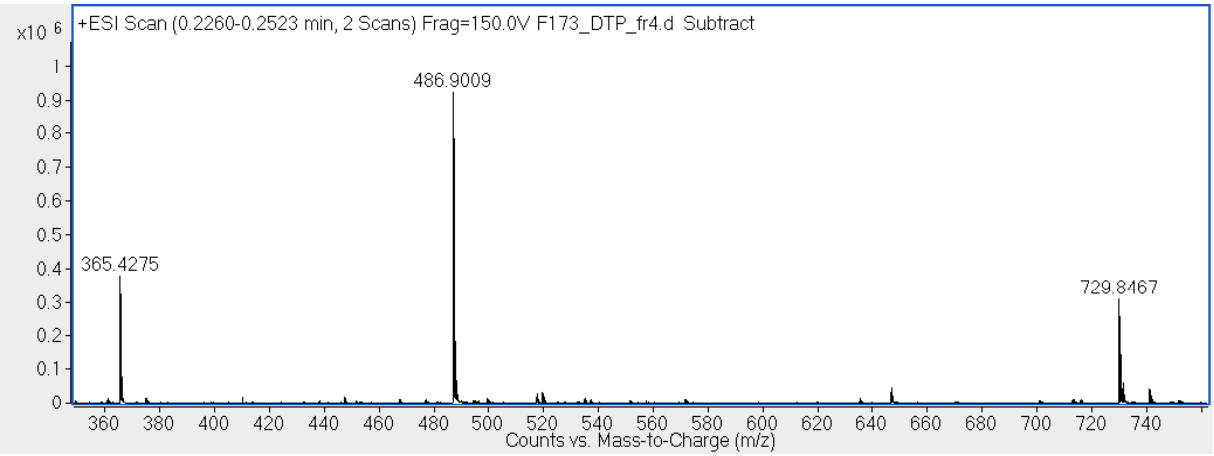

Figure S6: ESI-MS spectrum of SarTATE

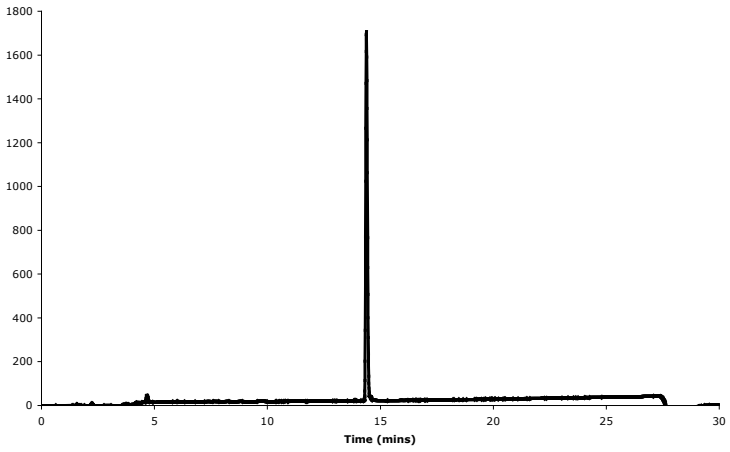

Figure S7: HPLC trace of SarTATE

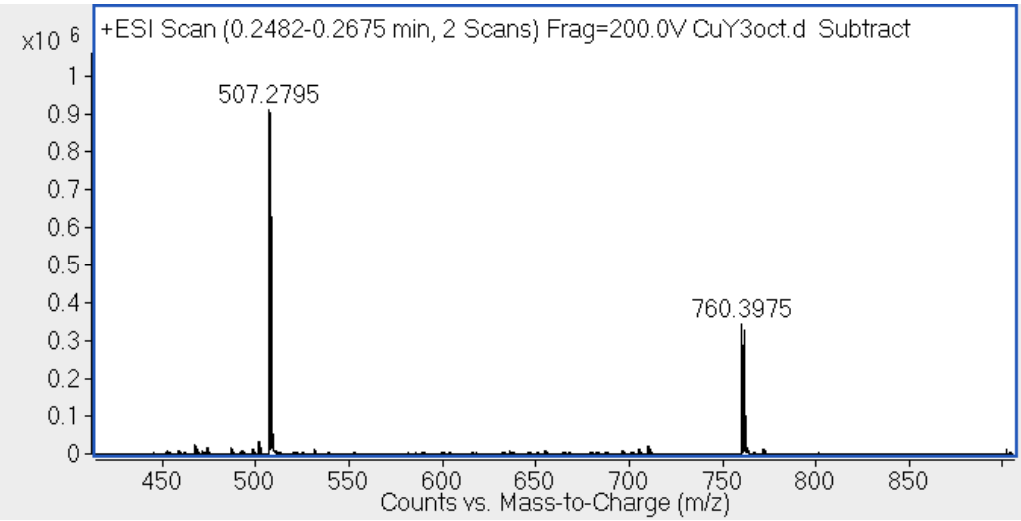

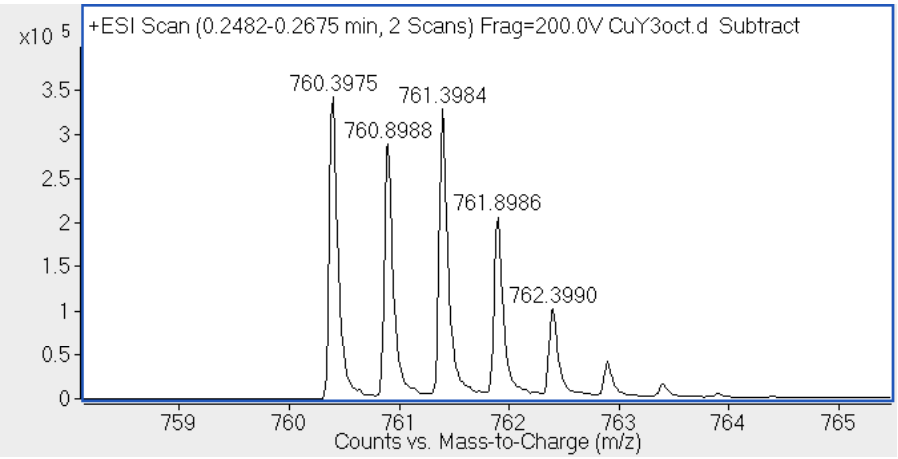

Figure S8: ESI-MS spectra of CuSarTATE

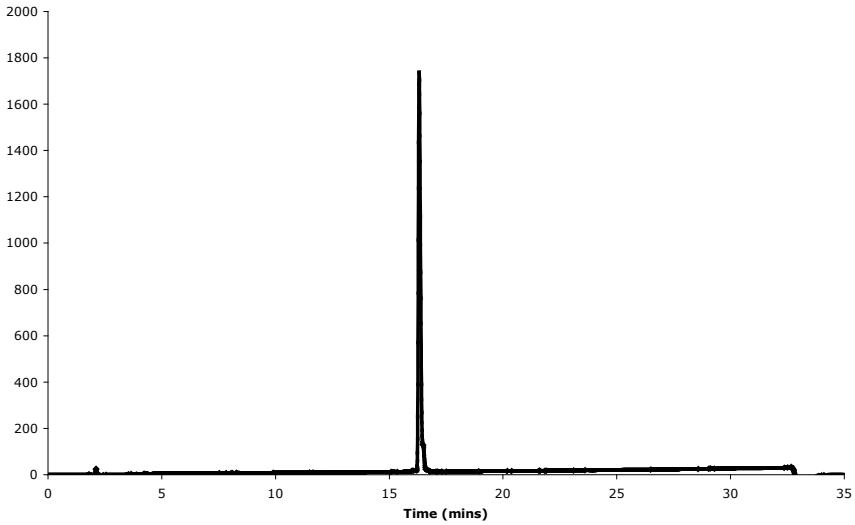

Figure S9: HPLC trace of CuSarTATE

Table 1. Crystal data for $[Cu(MeCOSar)](ClO_4)_2 \cdot 0.5CH_3CN$

Compound name	$[Cu(MeCOSar)](ClO_4)_2 \cdot 0.5CH_3CN$ (CCDC 915824)
Empirical formula	$C_{21}H_{42.5}C_{l2}CuN_{7.5}O_{11}$
Formula weight	710.57
Temperature/ K	130.0(1)
Wavelength/ Å	1.5418
Crystal system	monoclinic
Space group	*C*12/*c*1
a/ Å	15.5144(3)
b/ Å	8.9798(2)
c/ Å	42.7107(11)
α/ º	90.0
β/ º	94.906(2)
γ/ º	90.0
Volume/ $Å^3$	5928.5(2)
Z	8
Density (calculated) (g/cm^3)	1.592
Absorption coefficient (mm^{-1})	3.307
F(000)	2976
Reflections collected	11236
Independent reflections	5850 [*R*(int) = 0.0289]
Reflections with I > 2sigma(I)	4797
Refinement method	Full-matrix least-squares on F^2
Goodness-of-fit on F^2	1.110
Final R indices	[>2 sigma(I)] *R*1 = 0.0462, *wR*2 = 0.1078
R indices (all data)	*R*1 = 0.0603, *wR*2 = 0.1135

Table 2. Biodistribution results of ^{64}CuSarTATE in Balb/c mice bearing A427-7 tumour xenografts at 2 and 24 h post-injection. A blocking study was performed by co-injecting an excess of Tyr^3-octreotate (150 µg) to block the receptors. Results are expressed as percentage of injected dose per gram of tissue (%ID/g ± standard error) and represent the mean of 3 mice/tissue.

Organs	2 h	2 h blocking	24 h
Blood	0.40 ± 0.10	0.73 ± 0.19	0.11 ± 0.01
Lungs	1.15 ± 0.17	1.94 ± 0.41	0.65 ± 0.18
Heart	0.33 ± 0.03	0.80 ± 0.13	0.30 ± 0.05
Liver	3.12 ± 0.76	6.30 ± 0.93	1.71 ± 0.36
Kidneys	35.17 ± 3.14	47.69 ± 3.63	10.05 ± 2.00
Muscle	0.22 ± 0.07	0.40 ± 0.18	0.07 ± 0.004
Spleen	1.74 ± 0.62	2.77 ± 0.63	0.78 ± 0.11
Tumour	31.20 ± 7.54	5.89 ± 0.18	31.42 ± 8.11
Tumour-to-normal tissue ratio			
Tumour to blood	89.4 ± 34.1		307.0 ± 107.1
Tumour to muscle	167.2 ± 63.1		430.9 ± 129.6
Tumour to kidney	0.9 ± 0.3		3.8 ± 1.7
Tumour to liver	10.1 ± 1.0		22.7 ± 10.7

Table 3. Biodistribution results of ^{64}CuDOTATATE in Balb/c mice bearing A427-7 tumour xenografts at 2 and 24 h post-injection. Results are expressed as percentage of injected dose per gram of tissue (%ID/g ± standard error) and represent the mean of 3-4 mice/tissue.

Organs	2 h	24 h
Blood	0.64 ± 0.02	0.56 ± 0.04
Lungs	3.13 ± 0.54	3.09 ± 0.36
Heart	1.60 ± 0.19	1.53 ± 0.13
Liver	9.93 ± 1.16	5.91 ± 0.46
Kidneys	6.59 ± 0.55	3.49 ± 0.29
Muscle	0.29 ± 0.01	0.26 ± 0.03
Spleen	1.57 ± 0.15	1.51 ± 0.08
Tumour	27.75 ± 1.76	10.35 ± 1.36
Tumour-to-normal tissue ratio		
Tumour to blood	43.3 ± 1.7	18.4 ± 2.1
Tumour to muscle	96.0 ± 6.7	39.3 ± 4.0
Tumour to kidney	4.2 ± 0.4	2.9 ± 0.2
Tumour to liver	2.9 ± 0.3	1.8 ± 0.3